4 Examination of the Balance of Forces in the Vertical Magnetic Alignment of Microwire Ensembles

Silicon microwires with ferromagnetic coatings have been aligned into vertically oriented ensembles using the application of perpendicular magnetic fields. Ni and Co coatings have been deposited on Si microwire arrays with controllable and uniform thickness along the wire length. The magnetization response of these coatings has been studied by superconducting quantum interference device measurements. Variable alignment response has been observed by tuning the surface tension of the solvent used, as well the surface chemistries of the alignment substrate and the microwire itself. The impact of different surface energetic parameters has been studied empirically using atomic force microscopy. Absolute values of force for the adhesion of a single microwire have been measured to be on the order of 1–100 nN. A force balance model for the magnetic torque induced vertical alignment of microwires has been proposed. By using empirically derived values for magnetic and surface energetic parameters it is possible to use this model predictively for the determination of the necessary applied magnetic field to align nano- or microwires of arbitrary geometries. Understanding of this directed assembly process is valuable not only on a fundamental level, but for its ability to inform the fabrication of microwire array solar devices incorporating magnetic assembly of active absorber components.

4.1 Background and Introduction

High efficiency solar devices have been fabricated using arrays of vertically oriented Si microwires in place of conventional planar absorbers. By decoupling the directions of light absorption and minority charge carrier collection devices with efficiencies these devices can achieve efficiencies as high as 7.9% and peak absorption efficiencies as high as 96% while using significantly less Si. [5–7, 23, 24, 26] The result is a device that not only has a potentially lower cost of production but can be embedded in flexible polymer matrices, in comparison to current, rigid, planar Si cells. [25]

Unfortunately, these device designs, and the designs of many other electronic devices that incorporate periodic arrangements of oriented micro- or nanostructured elements rely on energy intensive cleanroom processes such as evaporation or photolithography. Additionally, some epitaxial growth processes are not amenable to the removal and manipulation of the fabricated elements from the substrate. However, colloidal methods are available for the synthesis of high-aspect ratio nano- and microcrystals composed of a range of materials, including metal oxides, [9] metal chalcogenides, [27] group III-V materials, [28] and elemental semiconductors. [10, 44, 45] These processes are highly scalable but produce a randomly oriented solution of particles. A self- or directed-assembly process to align the randomly oriented suspensions of microcrystals into the desired vertically oriented arrays would allow these scalable synthetic processes to be leveraged.

Self- and directed-assembly methods have been well-explored on the nanoscale, [46] and objects ranging from disks to rods have been assembled using electric- and magnetic field assisted assembly, [11, 12, 18, 19, 29, 47, 48] fluidic assembly, [34] Langmuir-Blodgett assembly, [14] and evaporation-induced self-assembly. [13, 20, 21, 30] These methods can be applied to create well-ordered arrays of a variety of metallic, semi-

conducting, and magnetic colloidal nanoparticles. Low-aspect ratio microstructures (aspect ratio ≤ 1) have likewise been studied, where particles such as spheres and platelets have been readily assembled through the use of surface energy interactions [15, 31] and externally applied fields. [16, 32, 33, 49] Relatively few techniques, however, exist for the alignment of micron sized high-aspect ratio structures, which is required for the preparation of solar cell devices incorporating anisotropic microstructures of indirect band gap semiconductors such as Si.

Recently, a directed assembly technique using magnetic fields to vertically orient high-aspect ratio ensembles of Si microwires over the cm^2 scale has been presented. [1] In this technique, Si microwires on the order of 100 μm long were coated with a thin layer of ferromagnetic Ni, aligned vertically into monolayers by the use of magnetic fields, and subsequently captured in polymer films. The degree of vertical alignment, and the minimum field strength required for alignment, were evaluated empirically as a function of geometric properties, such as microwire length and thickness of magnetically responsive Ni coatings, as well as surface energetic properties, such as substrate surface chemistry and alignment solvent choice.

In this study we develop a force balance model to examine the magnetic alignment process on a fundamental basis. Pertinent interfacial and magnetic forces are examinated with a mix of analytical and empirical techniques in order to inform the choice of system parameters, including surface derivatization, magnetic material deposition, and microwire geometry. In addition to adding to a fundamental understanding of magnetic field directed assembly at the microscale, this will enable greater efficiency in the fabrication of microwire array solar cells without the use of a clean room.

4.2 Theory

A predictive model has been developed for the vertical magnetic alignment of microwires. This allows for the prediction of the necessary magnetic field to align a microwire with the appropriate inputs of wire geometry, magnetic parameters, and surface chemistry of the wire and substrate. This model has been developed to examine the case of a single microwire and is shown schematically in Figure 9, with downward force represented in red and upward (vertically orienting) forces represented in green.

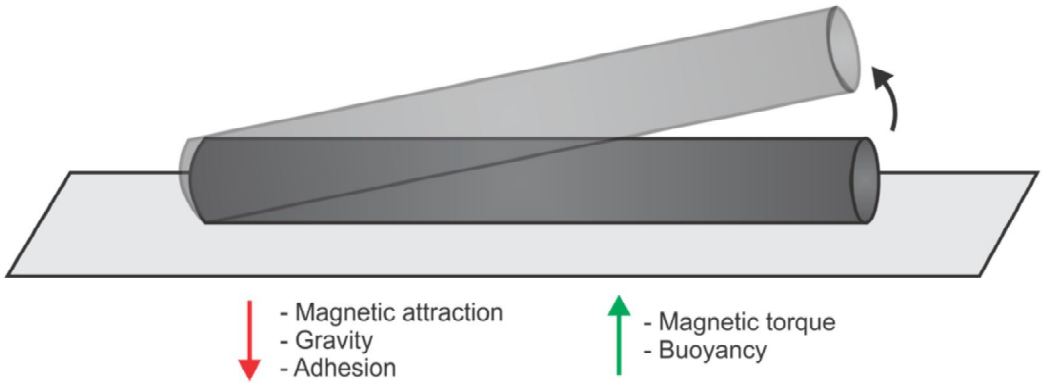

Figure 9: Schematic of magnetic alignment force balance.

This model assumes a single wire on a substrate in the presence of a magnetic field, and is therefore valid for sparsely distributed wires. If the microwires were in close contact then a dipole interaction term for the magnetic coupling would be necessary, however this was not included as the desired microwire array device in this study is comprised of non-contacting microwires. Additionally, a repulsive term can be introduced to overcome magnetic coupling forces by derivatizing the microwires with an ionic group, as described in Section 4.3.3.

This model also assumes that each wire when exposed to a perpendicular magnetic field twists up while retaining contact with the substrate at one end *via* van der Waals

interactions. This has been observed to be the case empirically. [1] Additionally, this implies that the microwires are relatively stationary with respect to their original lateral arrangement and that the only forces to be considered are those operating in the vertical direction. This lack of translation keeps the microwires isolated, and therefore prevents the magnetic coupling previously described.

4.2.1 Relevant Forces

Gravity and Buoyancy Gravitational forces (F_G) are represented in Equation 1, and are dependent on the total mass of the microwire and coating (m) as well as the downward acceleration due to gravity (g).

$$F_G = -m \cdot g \tag{1}$$

Buoyant forces (F_B) operate in the opposite direction and are given in Equation 2. Relevant parameters are the total microwire volume (V), and the density of the alignment solvent (ρ_S).

$$F_B = g \cdot \rho_S \cdot V \tag{2}$$

Surface Adhesion A term representing the force of surface adhesion (F_A) is necessary when a microwire on a substrate is pulled away from the surface and is given in Equation 3. This term is not necessary for a free-floating wire in solution.

$$F_A = \frac{-\Delta G_{132} \cdot A_I}{d} \tag{3}$$

The force of adhesion is an attractive force, assuming a substrate rather a superstrate, and is dependent upon the Gibbs free energy of adhesion (ΔG_{132}), the effective area of interaction between the microwire and the substrate (A_I), and the distance of closest approach between the microwire and substrate (d). The closest approach distance is

taken to be the van der Waals contact distance, or approximately 3 angstroms, for the base of the microwire cylinder coming into contact with the substrate. This assumes there are no ionic interactions or other forces and can vary depending on surface chemistry, material elasticity, surface roughness, microwire faceting, and other factors. The effective area of interaction takes into account that the surfaces in question are in fact not perfectly smooth but some microwire surface roughness (Figure 11) exists as well as substrate roughness. Similarly, the microwires can deviate from perfect cylinders with protrusions or other inhomogeneities, which can be captured in the effective area of interaction.

The Gibbs free energy of adhesion is described in Equation 4. The subscript term in the Gibbs free energy refers to the three components of the system: the microwire surface (1), the substrate surface (2), and the fluid medium they come into contact in (3). The Gibbs free energy of adhesion is the sum of the Gibbs free energy of the nonpolar, i.e., Lifshitz van der Waals, interactions (ΔG_{LW}) and the polar, i.e., acid-base, interactions (ΔG_{AB}). These values can be calculated using the individual surface and surface tension components of the system, as per the procedure described by van Oss et al. [50]

$$\Delta G_{132} = \Delta G_{LW} + \Delta G_{AB} \tag{4}$$

Due to the area of interaction term described in Equation 3, calculating the surface adhesion force can be difficult in case involving complex structured materials, incorporating surface roughness and other geometric complications, such as microwire faceting and asymmetry. Therefore, in this study an empirical method has been used to calculate surface adhesion forces on a per wire basis, which involves the use of atomic force microscopy and will be described in Section 4.3.3.

Magnetic Attraction Magnetic attractive forces (F_{MA}) are given in Equation 5 and are relevant in cases where the magnetic field gradient in the vertical direction (dH/dZ) is nonzero. Magnetic attraction is dependent upon the magnetically responsive volume of the microwire, i.e., the volume of the ferromagnetic shell (V_S). Lastly, magnetic attraction is dependent upon the magnetization constant of the microwire (M_W) at the given value of applied field. Determination of the magnetization constant is discussed in Section 4.3.1.

$$F_{MA} = -M_W \frac{dH}{dZ} \cdot V_S \tag{5}$$

For the purpose of these equations a negative value of magnetic attraction was used, representing a system with a permanent magnet installed below the alignment substrate. This magnet could also be installed above the sample plane in order to apply an upwards pulling force. In the case of an alignment performed inside an electromagnetic coil the gradient, and thus this whole term, will go to zero.

Magnetic Torque The Ni and Co deposited on the microwires are soft magnetic materials, as has been verified by SQUID measurements of the coercivity (Section 4.3.1). Coercivity is defined as the necessary applied field to return a magnetized volume to a zero magnetization state. Soft magnetic materials differ from hard magnetic materials (where the coercivity is high, and the material does not easily lose its magnetic orientation in an applied field) in that they cannot typically be treated by a simple dipole model, with the material rotating to match the external field. This is because the magnetization vector is a function of the field vector, rather than a constant. The magnetization angle ϕ as a function of the wire angle Θ is described in Equation 6, [51] where n_a and n_r are the axial and radial demagnetization components, respectively. The demagnetization components are a function of the aspect ratio of the microwire and have been calculated as described in the literature to be

$n_a = 0.002$ and $n_r = 0.499$ for typical lengths and radii of microwires, assuming an ellipsoidal shape. [51]

$$\phi = tan^{-1}\left(\frac{n_a}{n_r}\, tan\,\Theta\right) \tag{6}$$

In the case of the force balance for the microwires studied here, even though the applied field is near orthogonal to the easy axis of the microwires (the axial direction, which is most easily magnetized), due to their high aspect ratio the microwires will tend to magnetize along their axis independent of their angle with respect to the applied field. We can therefore treat them as dipoles, as would be the case with a hard magnetic material, due to their strong shape anisotropy, and calculate the magnetic torque straightforwardly.

The magnetic torque (T_M), represented in Equation 7, is a function of the microwire magnetization constant and is considered to be an upward force in the case of a microwire constrained to a sample surface. It would have no net vertical component in the case of a free-floating microwire.

$$T_M = M_W \cdot H \cdot sin\,\Theta \cdot V_S \tag{7}$$

The magnetic torque is additionally dependent on the applied field (H), as well as the magnetically responsive volume of the microwire. This equation assumes the case of a uniform distribution of magnetically responsive material in the axial direction, which has been verified by electron microscope cross sectional analysis. Finally, the magnetic torque is dependent on the angle (Θ) between the applied field vector and the axial direction of the microwire. This gives a maximum force when the microwires are flat on the substrate in the presence of a vertical magnetic field, as is the initial case in these experiments. It also acts as a restoring force to hold the microwires in a vertical configuration if they are perturbed after alignment.

4.2.2 Force Balance

The force balance model used is shown below in Figure 10. Conditions A and B describe an equilibrium situation where a magnetic field has been applied exactly equal to the sum of the other forces in the system. The net force and net torque of this system are therefore zero. Condition C describes the dynamic situation where the microwire has detached from the surface and is moving upwards towards alignment.

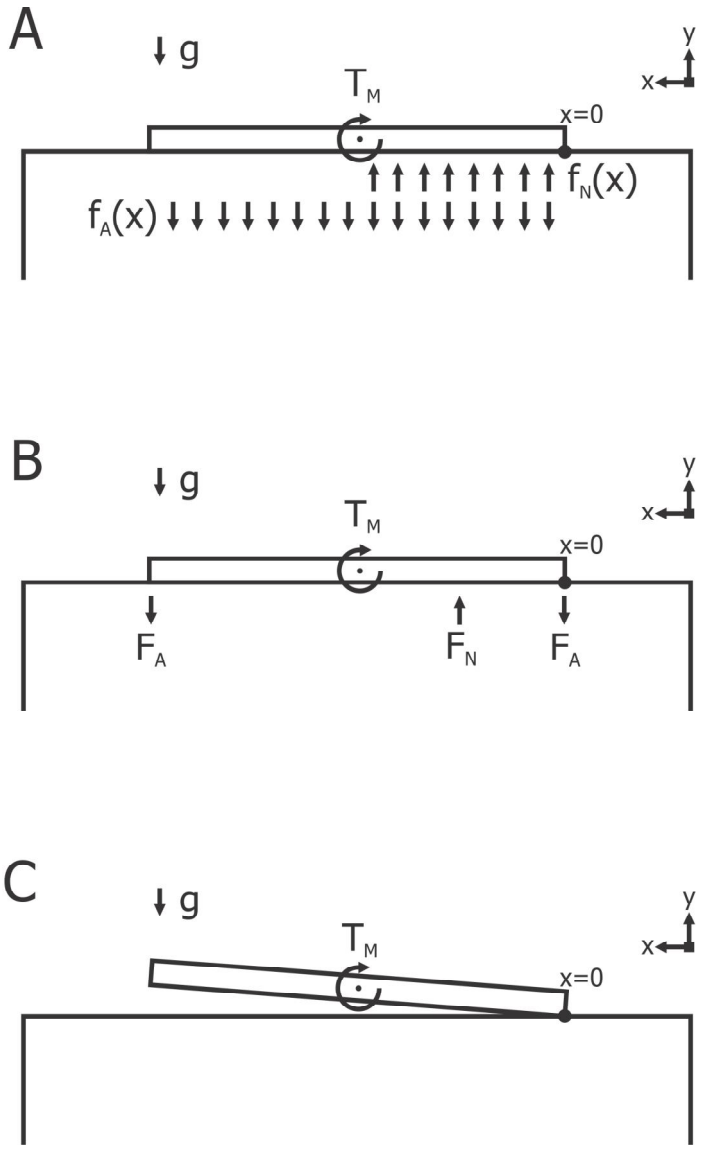

Figure 10: Detailed schematic of magnetic alignment force balance in (A) the surface attached condition, (B) the endpoint attached condition, and (C) the end attached condition.

Order of magnitude calculations were employed to determine the most relevant forces for this system, assuming a single microwire 100 μm in length, 2 μm in diameter, and with a 300 nm Ni shell. These forces are given on a per wire basis. Gravitational and buoyant forces were on the orders of 10^{-11} and 10^{-12} N, respectively. Magnetic attractive forces could be tuned over several orders of magnitude, depending on the strength of the applied field gradient. Surface adhesion forces were measured empirically to be on the order of 10^{-8} to 10^{-9} N. Gravitational and buoyant forces are relatively small and were therefore neglected for the purpose of this calculation, but would be straightforward to include as an additional distributed force component in the case of much larger wires. For the purpose of this force balance, the magnetic attractive forces are set to zero, as the majority of these experiments were carried out in the center of an electromagnetic coil, which has no net magnetic gradient. If this is not the case, another distributed force component can be added in the downward direction. Applying the force balance it becomes possible to solve for the minimum applied magnetic field necessary to align the wires vertically leveraging the force caused by magnetic torque. The force balance equation is given below (Equation 8), with distributed forces $f(x)$ representing per wire forces F normalized to wire length L. These equations follow the model for condition A in Figure 10.

$$\sum F_y = -f_A \cdot L + f_N \cdot \frac{L}{2} = 0 \tag{8}$$

$$f_N = 2f_A \tag{9}$$

This equation sets the sum of forces in the vertical y direction equal to zero in order to calculate the normal force f_N from the experimentally derived adhesion force f_A (as measured by AFM in Section 4.3.3). As shown in Figure 10, the wire is assumed to rotate around one fixed end, as observed to be the case empirically. The concentrated magnetic torque is assumed to operate at the center of the microwire, pulling

up on one half and pushing down into the substrate on the other. Therefore, the adhesion force term in the above equation is given for the entire wire length, and the normal force term is only considered for half of the wire length. This simplifies to yield Equation 9, where the normal force is calculated to be equal to exactly twice the surface adhesion force. Additional forces, such as the force of gravity, buoyancy, magnetic attraction, or ionic interactions would show up here if large enough to be significant.

Adding the torques due to normal and adhesion force and setting them equal to zero, as shown below in Equation 10, gives rise to the concentrated magnetic torque (T_M) to be solved for (Equation 11). This will allow the applied magnetic field H to be solved for, as it is directly proportional to magnetic torque.

$$\sum T_{x=0} = 0 \tag{10}$$

$$T_M + \int_0^{L/2} f_N(x)\, x \mathrm{d}x - \int_0^{L} f_A(x)\, x \mathrm{d}x = 0 \tag{11}$$

Substituting in the relationship for magnetic torque (Equation 7) and solving the integrals for the distributed torques gives Equation 12. Since the wires are radially symmetrical and uniform in dimensions along the axial direction, the integrals can be evaluated straightforwardly (Equation 13).

$$M_W \cdot H \cdot sin\,\Theta \cdot V_S + 2 f_A \frac{x^2}{2}\bigg|_0^{L/2} - f_A \frac{x^2}{2}\bigg|_0^{L} = 0 \tag{12}$$

$$M_W \cdot H \cdot sin\,\Theta \cdot V_S + f_A \left(\frac{L^2}{4} - \frac{L^2}{2} \right) = 0 \tag{13}$$

Simplifying the expression and substituting in the relationship of the cross sectional area of magnetic material A_S as equal to the magnetically responsive volume V_S normalized to length gives Equations 14 and 15.

$$M_W \cdot H \cdot sin\,\Theta \cdot V_S = f_A \cdot \frac{L^2}{4} \tag{14}$$

$$M_W \cdot H \cdot sin\,\Theta \cdot A_S = f_A \cdot \frac{L}{4} \tag{15}$$

Finally, substituting in the empirically derived adhesion F_A and rearranging the expression gives the necessary applied magnetic field H as a function of the experimentally determined parameters of surface force per wire (F_A) and magnetization (M_W). Since the magnetization is dependent upon applied magnetic field for materials below the saturation magnetization, it is necessary to solve this equation iteratively to find the actual value of magnetic field.

$$H = \frac{F_A}{4M_W \cdot A_S \cdot sin\,\Theta} \tag{16}$$

The process used to derive Equation 16 has assumed a distributed surface force arising from continuous contact along the length of the microwire. This would be the case for a uniform cylinder or prism, but experimentally microwires often have a small amount of material attached to the base, where the growth process was initiated. This protrusion can be seen in Figure 13. In this case we can use the model described in condition B of Figure 10, where the surface force is modeled as two points, one on each end where the microwire is in van der Waals contact with the surface. This derivation gives the same relation shown in Equation 16, with the difference that in condition B the measured value of F_A is independent of length, where in condition A there would be a linear dependence.

Assuming condition B holds, Equation 16 shows no dependence upon microwire length, as additional torque from a longer region of magnetically responsive material will be balanced by additional torque from surface adhesive interactions. However, experimental evidence shows a dependence upon length where alignment becomes more facile with longer microwires (Section 3.2.4). This is because this equation represents the minimum level of applied magnetic field necessary to reach an equilibrium with the surface adhesive forces. At this point the microwire is constantly detaching and reattaching reversibly. When the microwire is in the detached state however, the dynamic situation described in Figure 10C is the predicted case. At this point there are no adhesive forces and the microwire is free to rotate in solution solely under the influence of magnetic torque, which, as described in Equation 7, has a linear dependence upon length. Assuming that gravitational influences are negligible, this situation is identical to that of a free floating microwire, as the translation of the center of mass of the microwire due to its state of being constrained to the surface can be ignored.

Therefore, a relationship for the minimum field needed for alignment can be described as a relationship of experimentally measurable surface adhesion interactions and magnetization constants. This relationship applies for microwires and varies based on cross sectional area of the magnetic sheath, but is independent of length. When this threshold value of field is met however, longer microwires will experience more facile alignment in higher fields due to a linear dependence of torque upon length.

4.3 Results

4.3.1 Microwire Fabrication

Electrodeposition Figure 11 shows scanning electron micrographs (SEMs) of silicon microwire arrays that have been electroplated with nickel (panel A) and cobalt (panel B). The wires show conformal coatings of the respective ferromagnetic handle materials from top to bottom. The inset in panel A shows the cross section of one wire, with the lighter region corresponding to the nickel sheath. The inset in panel B shows a high magnification view of the cobalt coating, illustrating its surface roughness.

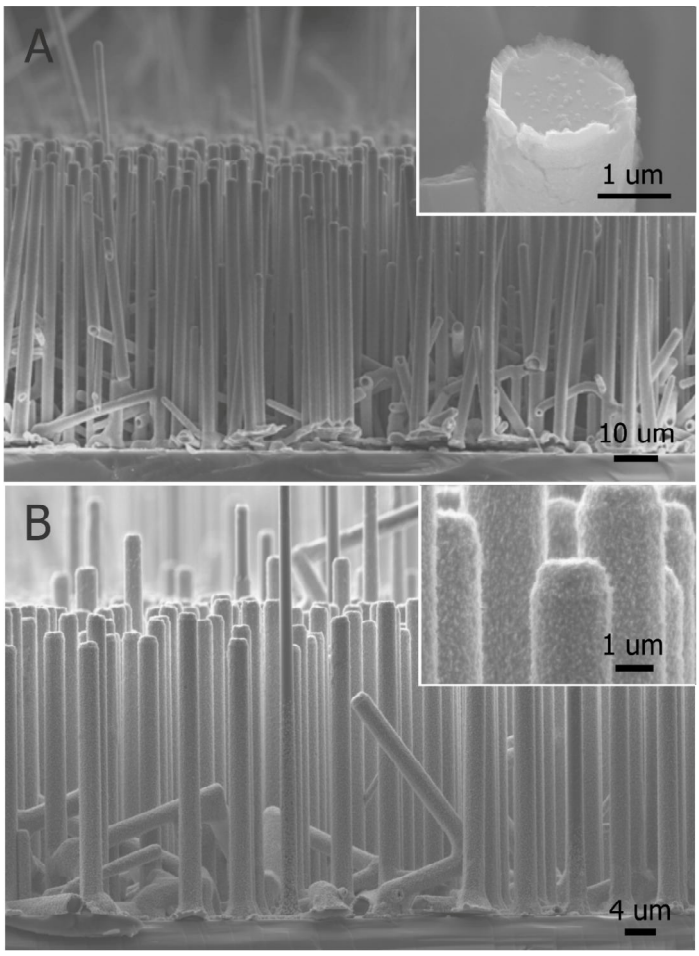

Figure 11: Electron micrographs of Si microwires plated with (A) nickel or (B) cobalt. Inset (A) shows cross section of coating. Inset (B) shows surface morphology.

SQUID Measurements Figure 12 shows example data for a superconducting quantum interference device (SQUID) measurement of an annealed, electrodeposited, Ni-coated Si substrate at 300 K. Measuring a SQUID hysteresis curve allows for the determination of magnetic moment and subsequently the magnetization of a sample at a range of applied field values. This hysteresis curve shows near magnetic saturation at an applied field in the range of 300 Oe, giving a magnetization value of 4.34×10^{-5} A m^{-1} at saturation.

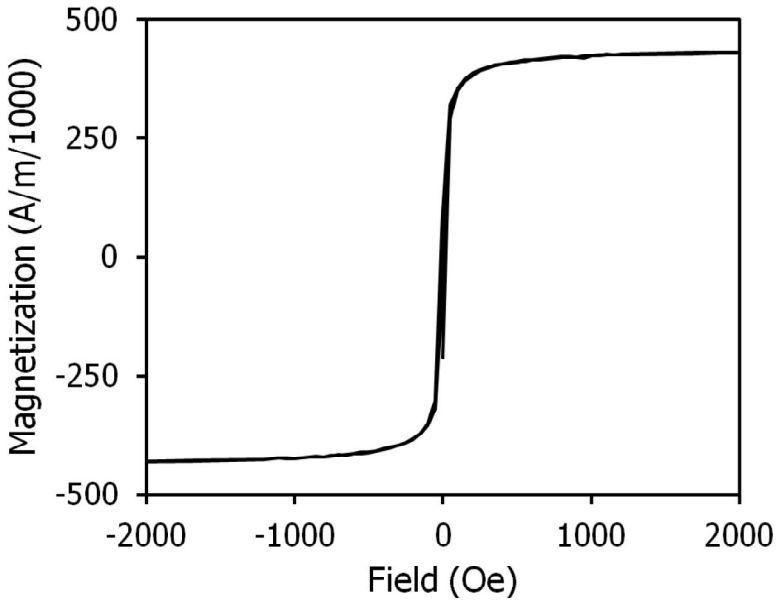

Figure 12: SQUID hysteresis curve of Ni electrodeposited on Si and subsequently annealed.

SQUID measurements were performed for both Ni and Co magnetic materials prepared using both sputter deposition and electrodeposition. Measurements were taken both before and after an annealing step in reducing environment. Table 1 summarizes these measurements. The values tabulated give the maximum magnetic saturation value recorded during each scan. With the exception of electrodeposited Co, most samples demonstrated an increase magnetization saturation following the annealing step. The values of Ni measured here are in agreement with literature recorded values. [22] Between the two materials, approximately an order of magnitude in magnetic response is spanned.

Material	**Deposition**	**As-Grown (A m^{-1})**	**Annealed (A m^{-1})**
Ni	Sputtered	2.59×10^5	3.29×10^5
Ni	Electrodeposited	4.11×10^5	4.34×10^5
Co	Sputtered	7.38×10^5	1.03×10^6
Co	Electrodeposited	5.70×10^5	4.90×10^5

Table 1: Magnetic saturation of Ni and Co films deposited by sputter deposition or electrodeposition, pre- and post-annealing.

4.3.2 AFM Tip Fabrication

Tipless atomic force microscope (AFM) cantilevers were modified with Si microwires of varying geometry and surface chemistry. This allows for the use of the microwires in place of a standard AFM tip. Figure 13 shows electron micrographs of two example tips. Above is a Si microwire coated with Ni, and below is a Si microwire that has been partially coated with Ni, modifying its surface adhesion properties. The microwires are attached orthogonal to the resonant direction of the cantilevers.

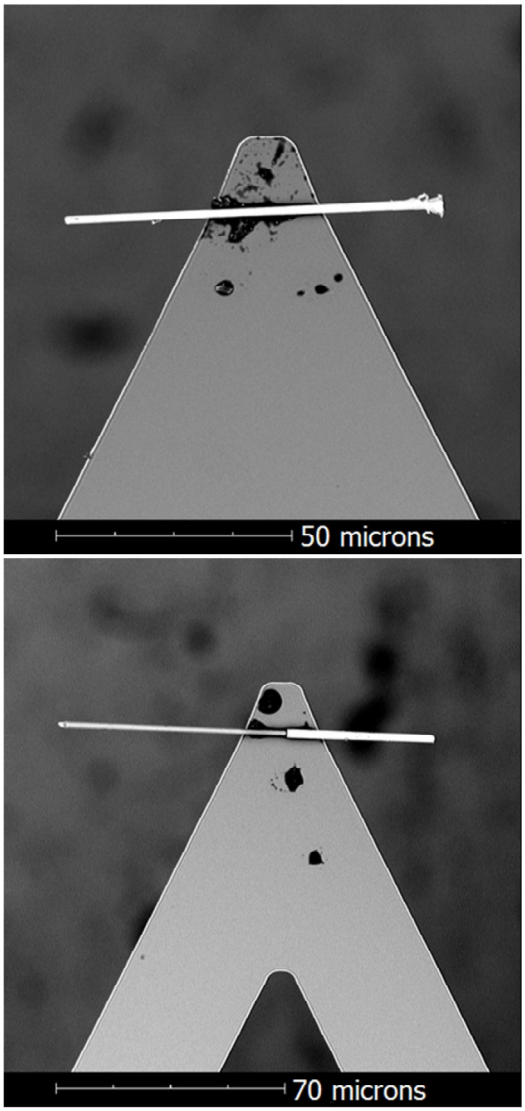

Figure 13: Electron micrographs of Si microwires attached to AFM cantilevers with epoxy. Two tips are shown, above is a uniformly plated microwire, below is a half-plated microwire.

4.3.3 Force Curve Measurements

Substrate and Solvent Dependence Figure 14 shows an AFM force curve acquired using a Si microwire approximately 75 μm long that has been electrodeposited with approximately 300 nm Ni and attached to a cantilever. Force curves were obtained using both a hydrophobic Si–H surface and a hydrophilic Si–OH surface. Only the retraction portion of the curve is shown, with 0 nm distance representing the tip forced into the surface. Upon retraction a region of negative (attractive) force is seen up until the tip disengages from the substrate at approximately 500 nm. The different between the peak attraction and baseline value represents a surface adhesion energy. In this plot the microwire exhibits less adhesion with the lower energy Si–H surface than with the Si–H surface.

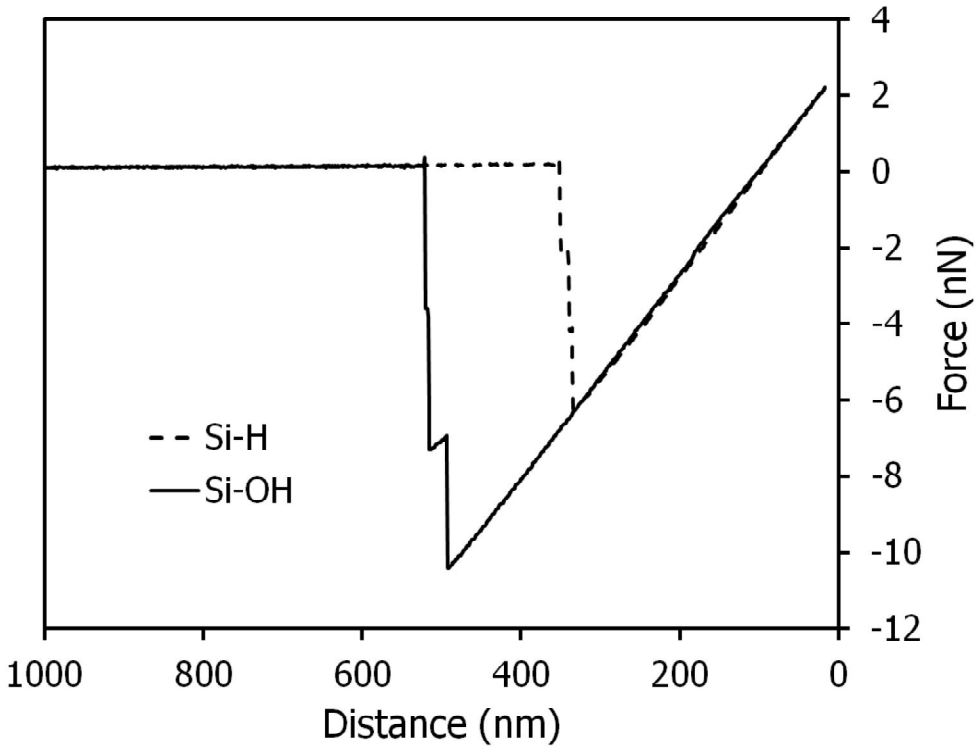

Figure 14: AFM force curves for a Ni-plated Si microwire in contact with a hydrophobic Si–H surface and a hydrophilic Si–OH surface in air.

Force curves were performed with a test Ni-plated Si microwire on Si–H and Si–OH substrates in the presence of both water and isopropanol in order to study the combined effect of substrate and solvent interactions on adhesion. Table 2 summarizes these results. Higher adhesion energies were observed from force curves run on the Si–H substrate than the Si–OH substrate, with the highest observed value from the Si–H/H_2O system. Lower adhesion energies were observed for systems incorporating isopropanol rather than H_2O.

Adhesion(nN)	**H_2O**	**Isopropanol**
Si–H	27.14	8.22
Si–OH	1.14	1.87

Table 2: Adhesion energies of the interaction between a test Ni-plated Si microwire and substrates of different surface energy in the presence of H_2O and isopropanol.

pH Dependence Figure 15 shows AFM force curves for a microwire that has been modified with carboxylic acid surface groups in contact with a Si substrate in the presence of aqueous solutions of HCl. At acidic conditions below the pKa of the carboxylic acid group a surface adhesion of approximately 3 nN is observed. At pH 6, where the carboxylic acid group is deprotonated into a carboxylate group, zero net adhesion is observed. This switching behavior persists when the solution pH is cycled back and forth around the pKa.

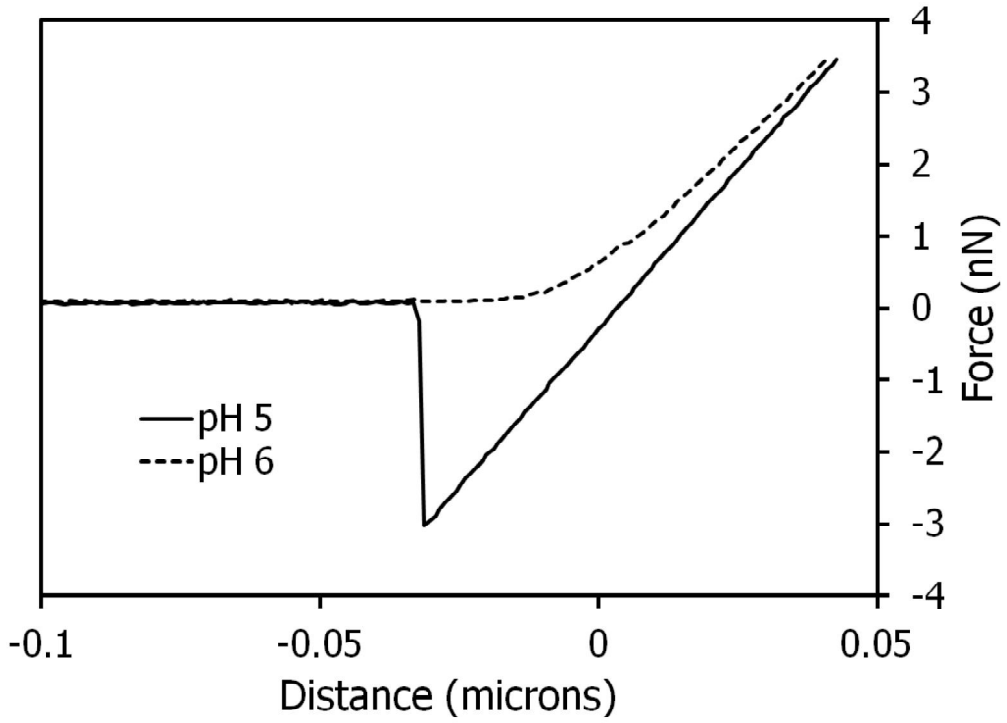

Figure 15: AFM force curve for a carboxylated Si microwire in contact with Si surface in solutions of pH 5 and pH 6.

Figure 16 shows the surface adhesion of a carboxylated Si microwire to a methylated Si substrate as a function of pH value. A chemically inert methylated substrate was used to exclude the effect of pH on a bare Si substrate. As in Figure 15, a switching behavior is seen between pH 5 and 6, where a stronger adhesion is seen when the carboxylic groups derivatizing the microwire tip are in their acidic form. The adhesion force is relatively constant in the acidic region of pH 2 to 5, and likewise relatively constant in the range of pH 6 to 13, where the carboxylic groups are in their carboxylate form.

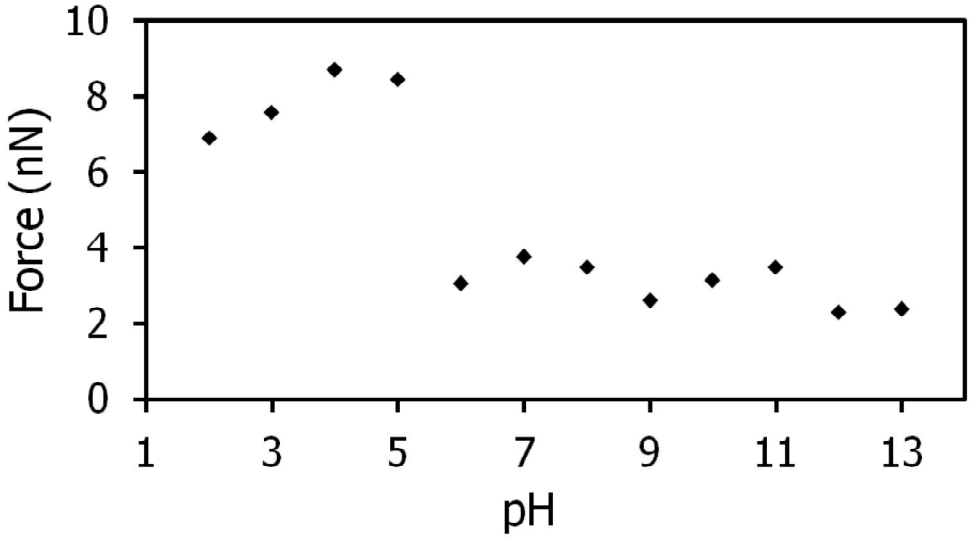

Figure 16: Plot of adhesion energies of a carboxylated Si microwire in contact with methyl-Si at different values of pH.

4.3.4 Force Balance Calculations

Figure 17 shows the predicted values of applied magnetic field for vertically aligning Si microwires as a function of radius. Traces are shown for combinations of different surface tension solvents (water and isopropanol) along with different surface energy substrates (Si–H and Si–OH). This plot assumes the model given in Section 4.2 and holds constant a Ni thickness of 185 nm. A decrease in magnetic field required is seen at larger values of radius. There is a strong, order of magnitude variation in the required field as a function of surface energy.

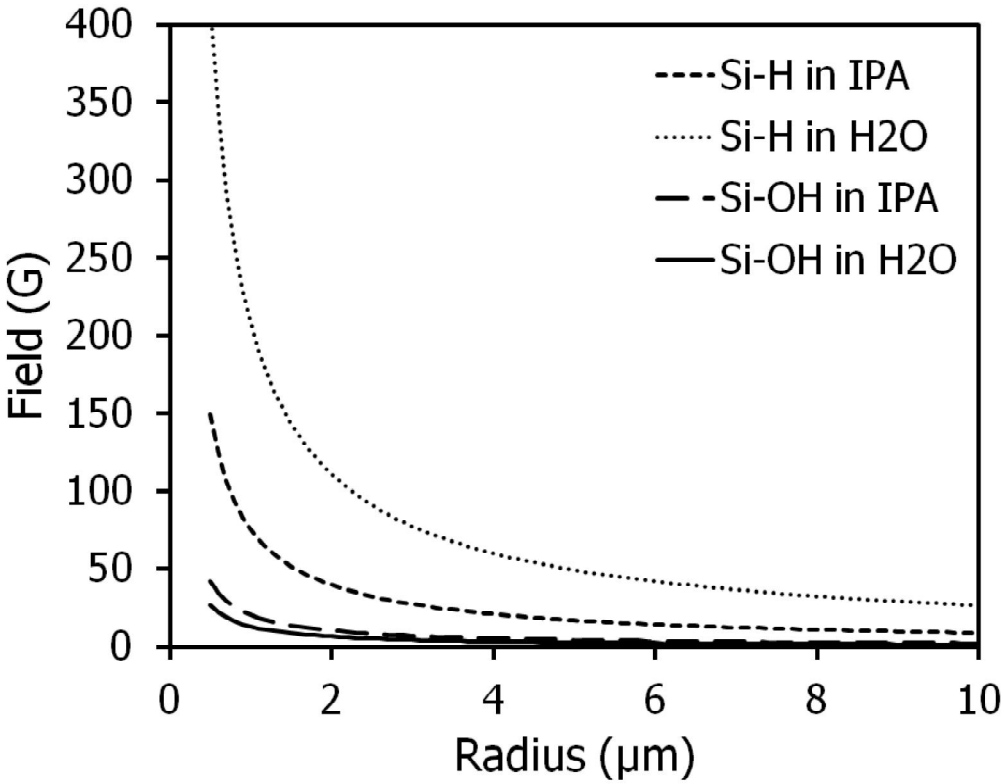

Figure 17: Plot of modeled magnetic field required for vertical alignment as a function of microwire radius, for different surface energetic combinations.

Figure 18 shows the torque developed for a free floating microwire depending on length. A linear relationship is observed where the torque increases for longer microwires and for higher values of applied magnetic field. This assumes that the microwires are free floating in solution and experience no surface interactions. Microwire radius was held at 0.95 μm and Ni thickness was 185 nm.

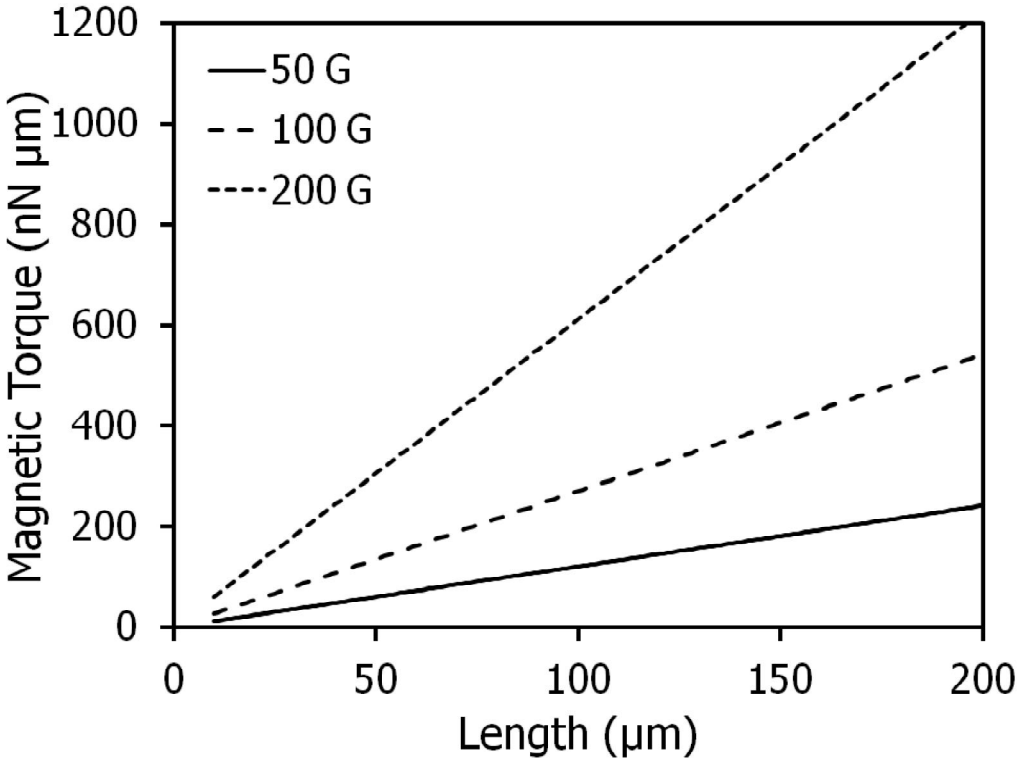

Figure 18: Plot of modeled magnetic torque applied to microwires as a function of length and applied magnetic field.

4.4 Discussion

4.4.1 Microwire Fabrication

Si microwires grown by the vapor-liquid-solid (VLS) chemical vapor deposition (CVD) process were chosen as a model system. [52] These microwires can be grown to highly controllable lengths and diameters, with good uniformity across the sample, [37] allowing for reproducible measurements of magnetic alignment. The Si microwires can be coated with either Ni or Co, as shown in Figure 11. Electrodeposition was chosen as the primary deposition method as it provides a more conformal coating than either sputter deposition or evaporation, leading to a microwire with a magnetic response that is uniform along the axial direction. Ni and Co were chosen to demonstrate broad applicability of the process for different material components, with different physical or magnetic properties. As seen qualitatively in the micrographs in Figure 11, the Ni coating is substantially smoother than the Co coating, which leads to a difference in surface adhesion interactions.

The magnetic properties of the Ni and Co sheaths were measured at room temperature using SQUID, with the results tabulated in Table 1. By a combination of deposition methods (electrodeposition and sputter deposition), and sample annealing, it possible to span approximately an order of magnitude in magnetic saturation response, from 2.59×10^5 to 1.03×10^6 A m^{-1}. On a per sample basis, the magnetic response to the applied field varies from zero to the saturation values listed previously. These SQUID measurements therefore give the pertinent magnetic constants for samples over the entire range of possible induced magnetic fields, allowing for accurate calculations of the magnetic attractive and torqueing force applied to a microwires required a wide range of different forces for alignment.

4.4.2 Force Curve Measurements

AFM Tip Fabrication AFM cantilevers with microwires attached as tips are presented in Figure 13. As can be seen in the electron micrographs, two types of microwires have been successfully attached to tipless cantilevers using chemically-resistant epoxy. The top image shows a fully Ni coated microwire and the bottom shows a microwire that has been partially coated *via* a polydimethylsiloxane (PDMS) "booting" step. [5] The microwires were attached with the minimum possible amount of epoxy in order to reduce any possible damping effect it would have on the cantilever during operation. These images demonstrate that microwires with varying dimensions and surface functionalities can be attached to cantilevers in order to probe substrate-microwire adhesion forces on a per wire basis.

This procedure has been modified from existing literature results for zero-dimensional colloidal particles, [53, 54] but the use one-dimensional particles is a novel extension of these techniques. The primary difference in attaching higher-dimensionality particles is the additional level of control that must be exerted over particle orientation. In this study, the microwires were attached with their primary axis orthogonal to the direction of resonance of the cantilever, so that the entire microwire contacts the substrate simultaneously, rather than one end coming into contact first.

Substrate and Solvent Dependence The magnetic alignment process is heavily dependent upon the choice of surface chemistry for the microwire and the substrate. In Figure 14 two force curves are given, representing the retraction of a cantilever tipped with a Ni plated Si microwire from two different substrates with varying surface energies. The difference between the in-air baseline at 0 nN and the point of highest attraction force represents the surface adhesion force. In this figure, the low surface energy Si–H substrate exhibits a lower force of attraction to the microwire

than does the high surface energy Si–OH substrate. Therefore, by modulated alignment substrate surface energy, magnetic alignment can be rendered more facile or difficult as desired.

In a vacuum (approximated by air in the above section) the lower surface energy substrate will provide the lowest adhesion energy to any choice of microwire surface energy. However, by performing the alignment in the presence of a fluid medium, hydrophobic interactions can be leveraged to make decrease adhesion strength on high surface energy substrates and enable facile magnetic alignment in these cases. This effect is displayed in Table 2. The presence of water and the polar solvent isopropanol yield higher adhesion energies for the lower surface energy Si–H substrate with the microwire tip than observed for the high surface energy Si–OH substrate. The effect is especially pronounced for the Si–H/H_2O/microwire system where the hydrophobic interactions are the strongest. In this case, hydrophobic interactions are broadly defined as the energy difference between the energy of the solvent-substrate and solvent-microwire interfaces when the substrate and microwire are not in contact and the energy of the substrate-microwire interface when they are. A high surface tension solvent such as water yields a large energetic penalty for separating two surfaces, and thus a hydrophobic effect is seen where objects tend to coalesce. This effect can be seen with a number of different solvents and substrates, including cases where water promotes individual particle solvation, so the term "hydrophobic effect" is used here only as a broad descriptor. In this system, modulating these parameters gives a wide range of adhesion energies, from $\sim$1-30 nN.

This AFM measurement, when properly calibrated, yields an absolute value of force which is a direct measure of an adhesion force that can be compared to magnetic fields required for vertical alignment of microwire ensembles. Performing these mea-

surements informs the choice of solvents and substrate/microwire surface chemistries, thereby giving a high degree of control over the magnetic alignment process, either for device applications or fundamental studies.

pH Dependence In addition to modifications in surface tensions or static surface energies, chemically responsive surface derivatizations can be used in order to add additional degrees of control to a system. In Figure 15 the effects of modifying a Si microwire with a carboxylic acid group are shown, where there is an abrupt change in surface adhesion force as a function of pH. At values of pH 5 and lower a pronounced surface adhesion is seen. This is below the pKa of the carboxylic group where it is in the acidic form. At values of pH 6 and higher, where the carboxylic groups are in their carboxylate forms, no net surface adhesion is observed. This switching behavior has been observed and is reproducible when cycling repeatedly between pH regions. This behavior is likely amplified by the choice of a bare, unmodified Si substrate for the force curve measurements. At low values of pH the native oxide of the Si will tend to strip, leaving behind a low surface energy hydride terminated surface. At high values of pH a hydroxyl layer will form at the surface of the Si giving a higher surface energy, and ultimately a strong repulsion to the negatively charged carboxylate groups as the Si–OH surface groups become deprotonated.

The same measurement was performed on methyl Si, a chemically inert Si surface modified by methyl groups *via* Grignard chemistry (Section 4.6.1) using carboxylated wires. The results of this measurement from pH 1 to 13 are given in Figure 16. As was the case previously, a higher value of adhesion strength is seen at pH 5 and below. However, in this case a net attraction is still observed at pH 6 and higher, though it is significantly reduced from the values from the more acidic conditions. In either regime, the values of adhesion are relatively constant, implying that the difference

in chemical state of the carboxylic group is primarily responsible for changes in adhesion behavior. Without the secondary effect of the Si substrate surface chemistry the difference in adhesion strength is not as large between the two pH regions, as would be expected from the relative differences in surface energy of the two systems at different values of pH.

This phenomenon can be leveraged in order to aid uniform magnetic alignment of microwire arrays. As discussed previously, microwires when in sufficiently close contact tend to couple magnetically and form large multi-wire agglomerates. Adding in a longer range ionic repulsion term by derivatizing the microwires with like charges may enable a stabilization of more closely spaced microwire arrays. This may enable efficient self-assembly of magnetic particles either with or without an external field by establishing a balance of ionic repulsion and magnetic attraction between appropriately functionalized and magnetized particles.

4.4.3 Force Balance Calculations

The plot in Figure 17 shows a dependence of magnetic field required for alignment upon the radius of the microwire, where larger radii microwires were easier to align. This is due to the additional magnetic material that would be present for a larger microwire with more magnetically responsive material. Different traces for various combinations of solvent surface tension and substrate surface energy are shown, with the necessary constants derived from AFM measurements. Assuming a microwire with a radius of 1 μm, as were used in experiments described in Section 3, the predicted values of magnetic field required for alignment show good order of magnitude agreement with the experimentally observed required magnetic fields. The plot described here represents the field required to bring the microwire into a zero net force and torque condition, where it is in a state of detaching and reattaching to the surface

continuously. Once the microwire is detached however, it comes under the influence of the magnetic torque of a free floating wire in solution, as described in Section 4.2.2. The magnetic torque on a microwire is shown in Figure 18 to be linearly dependent upon microwire length and applied magnetic field. This matches experimental observations of greater facility of alignment for longer microwires with increasing values of field (Section 3.2.4).

4.5 Conclusions

Magnetic alignment of microwires into vertical arrays for solar cell applications had been demonstrated, but was lacking a fundamental description of the physical chemistry involved. A model has been presented here which describes the alignment process as a function of microwire geometry, magnetization constants and surface interfacial interactions. The magnetization constants have been measured using SQUID, and the surface adhesion forces for a variety of systems have been obtained empirically using AFM with cantilevers modified with single microwires. This model shows order of magnitude agreement with experimental observations and can be used as a predictive model for the magnetic alignment of a range of microparticle systems.

4.6 Experimental

4.6.1 Sample Fabrication

Silicon Microwires Silicon wires ranging from 40–100 μm in length were fabricated by the vapor-liquid-solid (VLS) growth technique through the use of an in-house reactor. [37, 52] Cu-catalyzed microwires were grown at 1000 °C using $SiCl_4$ as a precursor, BCl_3 as a p-type dopant, and H_2 as a carrier gas. Growth times were between 10 and 40 min, with the longer growth times producing longer Si microwires. This process is described in detail in Section 3.6.1.

Electrodeposition For most samples, Ni and Co were deposited on the microwires electrochemically, to produce a ferromagnetic handle for alignment. The Si microwire arrays were first etched in buffered hydrofluoric acid (Transene, used as received), immediately prior to electrodeposition of the metal films. A commercial boric acid-buffered Ni sulfamate solution (Transene, used as received) served as the electroplating bath for the Ni films. The Co plating bath consisted of 1 M $CoSO_4 \cdot 7H_2O$, 45 g L^{-1} HBO_3, and 0.375 g L^{-1} sodium dodecyl sulfate (Sigma Aldrich, used as received). [55] All of the films were deposited on p-type (resistivity < 0.005 Ω cm) Si microwires at room temperature in a stirred, three-electrode electrochemical cell, at -1 V *vs.* a Ag/AgCl reference electrode. A platinum mesh was used as the counter electrode for Ni depositions, and a cobalt coil was used for Co depositions. The thickness of the coatings were systematically varied from approximately 100 nm to 500 nm by adjusting the deposition time from 5 min to 15 min. The resulting film thicknesses depended linearly on the growth time.

Sputter Deposition For the SQUID samples, Ni or Co were sputtered from 99.999% pure targets (Kurt J. Lesker, used as received) using a home-built RF magnetron sputter deposition system. In the sputtering process, materials were deposited at

$\sim$100 W forward power in an atmosphere of 1 mTorr Ar, from a base pressure of $< 1 \times 10^{-6}$ Torr, with resulting coating thicknesses between 20 and 300 nm.

AFM Tips Si microwires were attached to tipless SiN cantilevers (Bruker NP-O) using epoxy (Hysol 9460), following procedures adapted from previous literature for the attachment of zero-dimensional particles to AFM cantilevers. [53,54] A submicron tungsten microprobe tip (Micromanipulator Inc.) was used to transfer a dot of epoxy to the end of a cantilever under an optical microscope. A second microprobe tip was used to transfer a microwire to the epoxy dot. For nonmagnetic microwires capillary forces were used for the transfer, i.e., the microprobe tip was pressed into the target microwire until it adhered. For microwires with a magnetic coating, a microprobe tip with a magnetized, sputter-deposited, Ni coating was used to effect the transfer to the cantilever. Tips modified in this manner were cured overnight before transfer to ensure good adhesion of the microwire to the cantilever.

Silicon Surface Modification AFM substrates were rendered hydrophobic by a 2 min etch in buffered hydrofluoric acid (Transene, used as received), or hydrophilic by the same hydrofluoric acid etch followed by a UV/ozone treatment for 30 min in a ProCleaner UV/ozone system. These treatments yielded surfaces referred to as Si–H and Si–OH, respectively. The substrates were degreased with isopropanol prior to treatment. Methylated Si substrates were prepared as described in previous literature. [56] Si microwires were functionalized with decanoic acid terminations using a hydrosilyation protocol reported previously. [57] Briefly, as-grown Si microwires were etched in hydrofluoric acid for 30 s, followed by rinsing in deionized water. Samples were functionalized using a solution of 10% undecylenic acid (Aldrich, $>$ 95%, used as received) in toluene under UV radiation (254 nm, 5 hours) in a quartz glass reactor under inert atmosphere.

4.6.2 Characterization

Microscopy The dimensions of the wires were measured using a ZEISS 1550 VP field emission scanning electron microscope. Cross sections of the as-grown arrays were imaged before and after deposition, and the length and width measurements were obtained by averaging over 5–10 wires per sample. Electron micrographs of custom AFM tips were acquired using a Phenom Pro scanning electron microscope.

Microwires were aligned in the center of a liquid-cooled solenoid electromagnet (fabricated in-house) that had field strengths that varied from 1 G to 1.5 kG. The field direction was oriented along the substrate normal. The electromagnet was installed below the objective of an Olympus BX-51 microscope that was equipped with a CCD camera that recorded video at 5 frames per second. A Keithley source meter controlled by LabTracer software was used to power the magnetic field sweep. The magnetic field strength was calibrated to the power applied to the electromagnet using a Bell 5180 gaussmeter, with magnetic fields stable to within $\pm$ 1 G over the course of a typical experiment.

SQUID Measurements The magnetic properties of the deposited metal films were characterized using a Quantum Design superconducting quantum interference device. Hysteresis curves of Ni and Co films were obtained at 300 K from -8 to 8 tesla, and were normalized to the deposited thickness of material to obtain values for magnetization. Samples were measured immediately after fabrication to exclude aging effects.

AFM Force Curves Force curve measurements were conducted using a Bruker Dimension Icon atomic force microscope equipped with a liquid probe holder. A custom fluid cell was used to contain the analysis fluid and sample substrate. Force

curves were measured in Quantitative Nanomechanical Mapping Mode with typical ramp sizes in the range of 500 to 2000 nm. Typical PeakForce setpoints used were in the range of 0.5 to 2 V. Several force curves were measured per position to ensure reproducible results. Deflection sensitivity was measured against the Si substrate itself. The thermal tune process in the provided Bruker analysis software was used to tune the custom cantilevers used and obtain spring constants for force calibration. Following cantilever calibration, solutions and substrates were exchanged as necessary for all measurements before the cantilever was removed or adjusted.